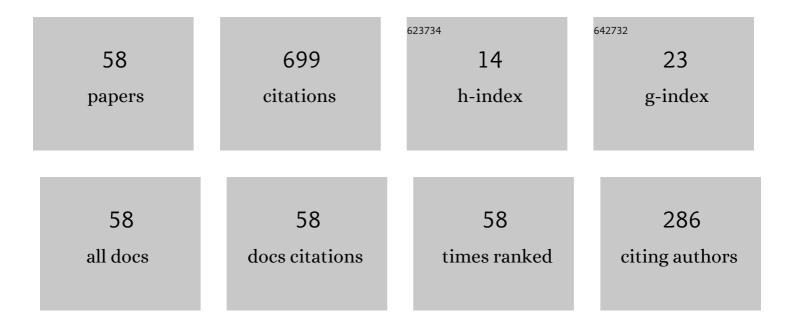
Jie-Ren Yang

List of Publications by Year in descending order

Source: https://exaly.com/author-pdf/3170553/publications.pdf Version: 2024-02-01



#	Article	IF	CITATIONS
1	Phase selection and solidification path transition of Ti–48Al–xNb alloys with different cooling rates. Rare Metals, 2023, 42, 288-295.	7.1	3
2	Investigation on microstructure and mechanical properties of heat-treated Ti-47.5Al–3Nb-3.5Cr alloy. Materials Science & Engineering A: Structural Materials: Properties, Microstructure and Processing, 2022, 832, 142366.	5.6	3
3	Phase transformation pathway and microstructural refinement by feathery transformation of Ru-containing Î ³ -TiAl alloy. Journal of Materials Research and Technology, 2022, 18, 5290-5300.	5.8	6
4	Thermomechanical instability and deformation behavior of βo(ω) phase region in a Ti-43Al-8Nb-0.2W-0.2B alloy under high-temperature rotary-bending fatigue. International Journal of Fatigue, 2022, 163, 106933.	5.7	2
5	Fabrication and Microstructure Optimization of TiAl Castings Using a Combined Melting/Pouring/Heat Treatment Device. International Journal of Metalcasting, 2021, 15, 890-898.	1.9	3
6	Active Eutectoid Decomposition of α → γ + τ1 and the Morphological Evolution in a Ru-Cont Acta Metallurgica Sinica (English Letters), 2021, 34, 1042-1050.	aining TiAl	Ąloy.
7	Microstructure refinement assisted by $\hat{I}\pm$ -recrystallization in a peritectic TiAl alloy. Journal of Materials Research and Technology, 2021, 11, 1135-1141.	5.8	7
8	Microstructure evolution and mechanical properties of a novel γ′ phase-strengthened Ir-W-Al-Th superalloy. Rare Metals, 2021, 40, 3588-3597.	7.1	5
9	The phase transformation behavior between γ lamellae and massive γ in a Ta containing TiAl-based alloy. Journal of Alloys and Compounds, 2020, 821, 153290.	5.5	11
10	Determination of Constitutive Equation and Thermo–Mechanical Processing Map for Pure Iridium. Metals, 2020, 10, 1087.	2.3	5
11	Continuous-Cooling-Transformation (CCT) Behaviors and Fine-Grained Nearly Lamellar (FGNL) Microstructure Formation in a Cast Ti-48Al-4Nb-2Cr Alloy. Metallurgical and Materials Transactions A: Physical Metallurgy and Materials Science, 2020, 51, 5285-5295.	2.2	16
12	Creep-Induced Phase Instability and Microstructure Evolution of a Nearly Lamellar Ti–45Al–8.5Nb–(W,) Tj E	т <u>д</u> д0 0 0	rgBT /Overlo
13	Grain refinement of 1 at.% Ta-containing cast TiAl-based alloy by cyclic air-cooling heat treatment. Materials Letters, 2020, 274, 127940.	2.6	17
14	An ultra-refining microstructure in rapidly solidified Ti–45Al-8.5Nb-(W, B, Y) alloy after an isothermal heat treatment. Journal of Alloys and Compounds, 2020, 827, 154283.	5.5	8
15	Evolution of Metastable α ₂ Phase in a Quenched Highâ€Nb ontaining TiAl Alloy at 800 °C. Advanced Engineering Materials, 2020, 22, 1901539.	3.5	2
16	In-situ observation of microstructure evolution and phase transformation under continuous cooling in Ru-containing TiAl alloys. Materials Characterization, 2020, 163, 110296.	4.4	11

17	Influence of heat treatment on microstructure and nanohardness of TiAl alloy solidified under high pressure. China Foundry, 2020, 17, 435-440.	1.4	0
18	Effects of Ru content on phase transformation and compression property of cast TiAl alloys. China Foundry, 2020, 17, 393-401.	1.4	5

JIE-REN YANG

#	Article	IF	CITATIONS
19	Refinement of massive γ phase with enhanced properties in a Ta containing γ-TiAl-based alloys. Scripta Materialia, 2019, 172, 113-118.	5.2	42
20	Phase Transformation and Fine Fully Lamellar (FFL) Structure Formation in a High Nbâ€Containing Betaâ€Gamma TiAl Alloy. Advanced Engineering Materials, 2019, 21, 1900244.	3.5	3
21	A Newly Generated Nearly Lamellar Microstructure in Cast Ti-48Al-2Nb-2Cr Alloy for High-Temperature Strengthening. Metallurgical and Materials Transactions A: Physical Metallurgy and Materials Science, 2019, 50, 5839-5852.	2.2	23
22	Microstructure Evolution and Mechanical Properties of Novel γ/γ′ Two-Phase Strengthened Ir-Based Superalloys. Metals, 2019, 9, 1171.	2.3	0
23	Effect of temperature gradient on competitive growth behavior of Si and YSi2 in a Si–Y eutectic alloy prepared by Bridgeman method. Ceramics International, 2019, 45, 16776-16783.	4.8	3
24	On the eutectoid decomposition of α→γ+τ1 in a Ru-containing TiAl alloy. Journal of Alloys and Compounds, 2019, 790, 42-47.	5.5	8
25	Molecular dynamics simulation and micropillar compression of deformation behavior in iridium single crystals. Rare Metals, 2019, , 1.	7.1	0
26	Continuous cooling transformationÂ(CCT) behavior of a high Nb-containing TiAl alloy. Materialia, 2019, 5, 100169.	2.7	13
27	Microstructure evolution and mechanical properties of a Ti-45Al-8.5Nb-(W, B, Y) alloy obtained by controlled cooling from a single β region. Journal of Alloys and Compounds, 2018, 740, 1140-1148.	5.5	25
28	Nucleation behavior of ï‰o phase in TiAl alloys at different elevated temperatures. Journal of Materials Science, 2018, 53, 5287-5295.	3.7	5
29	Numerical calculation and experimental evaluation of counter-gravity investment casting of Ti-48Al-2Cr-2Nb alloy. International Journal of Advanced Manufacturing Technology, 2018, 96, 3295-3309.	3.0	6
30	A Combined Electromagnetic Levitation Melting, Counterâ€Gravity Casting, and Mold Preheating Furnace for Producing TiAl Alloy. Advanced Engineering Materials, 2018, 20, 1700526.	3.5	8
31	Competitive growth of Si and YSi2 phases in a eutectic Si-Y alloy prepared by the Bridgeman method. Ceramics International, 2018, 44, 13232-13239.	4.8	6
32	Mechanical properties of an aged Ni-Cr-Mo alloy and effect of long-range order phase on deformation behavior. Materials Science & Engineering A: Structural Materials: Properties, Microstructure and Processing, 2018, 731, 29-35.	5.6	8
33	Anomalous Tensile Strength and Fracture Behavior of Polycrystalline Iridium from Room Temperature to 1600 °C. Advanced Engineering Materials, 2018, 20, 1701114.	3.5	3
34	Optimization of electromagnetic energy in cold crucible used for directional solidification of TiAl alloy. Energy, 2018, 161, 143-155.	8.8	13
35	High-temperature rotary-bending fatigue characteristics of a high Nb-containing beta-gamma TiAl alloy. Materials Science & Engineering A: Structural Materials: Properties, Microstructure and Processing, 2018, 735, 40-48.	5.6	14
36	Evolution of B2(ω) region in high-Nb containing TiAl alloy in intermediate temperature range. Intermetallics, 2017, 82, 32-39.	3.9	30

Jie-Ren Yang

#	Article	IF	CITATIONS
37	The Effect of Pressure Stress on the Evolution of B2(ω) Phase in High Nb Containing TiAl Alloy. Advanced Engineering Materials, 2017, 19, 1600844.	3.5	7
38	Numerical and experimental study of electron beam floating zone melting of Iridium single crystal. Journal of Materials Processing Technology, 2017, 250, 239-246.	6.3	9
39	Atomic-scale observations of B2 → ï‰-related phases transition in high-Nb containing TiAl alloy. Materials Characterization, 2017, 130, 135-138.	4.4	14
40	Tailoring the Microstructure of a β-Solidifying TiAl Alloy by Controlled Post-solidification Isothermal Holding and Cooling. Metallurgical and Materials Transactions A: Physical Metallurgy and Materials Science, 2017, 48, 5095-5105.	2.2	32
41	Evolution of Σ3n CSL boundaries in Ni-Cr-Mo alloy during aging treatment. Materials Characterization, 2017, 134, 379-386.	4.4	9
42	Microstructure Evolution in the Mushy Zone of a βâ€ 5 olidifying TiAl Alloy under Different Cooling Processes. Advanced Engineering Materials, 2016, 18, 1667-1673.	3.5	5
43	Precipitation of two kinds of γ laths in massive γ coexisting with γ lamellae in as-cast Ta-containing TiAl-Nb alloys. Materials Letters, 2016, 185, 480-483.	2.6	7
44	Temperature distribution in bottomless electromagnetic cold crucible applied to directional solidification. International Journal of Heat and Mass Transfer, 2016, 100, 131-138.	4.8	14
45	Microstructure control of Ti 45Al 8.5Nb (W, B, Y) alloy during the solidification process. Acta Materialia, 2016, 112, 121-131.	7.9	62
46	Transition of solidification path in nonequilibrium solidification of Ti–48Al–8Nb alloy. Rare Metals, 2016, 35, 48-53.	7.1	0
47	Effect of mold temperature and casting dimension on microstructure and tensile properties of counter-gravity casting Ti-6Al-4V alloys. China Foundry, 2016, 13, 9-14.	1.4	3
48	In-situ investigation on the β to α phase transformation in Ti–45Al–8.5Nb–(W, B, Y) alloy. Journal of Alloys and Compounds, 2016, 663, 594-600.	5.5	39
49	Solidification microstructure characteristics of Ti–44Al–4Nb–2Cr–0.1B alloy under various cooling rates during mushy zone. Rare Metals, 2016, 35, 35-41.	7.1	9
50	Effects of thermal history on the microstructure evolution of Ti-6Al-4V during solidification. Journal of Materials Processing Technology, 2016, 227, 281-287.	6.3	12
51	An atomic study of the transitional region between γ/γ laths in γ-TiAl. Intermetallics, 2015, 60, 13-18.	3.9	7
52	Response of the solidification microstructure of a high Nb containing TiAl alloy to an isothermal high-temperature heat treatment. Intermetallics, 2015, 63, 1-6.	3.9	29
53	Mechanism and evolution of heat transfer in mushy zone during cold crucible directionally solidifying TiAl alloys. International Journal of Heat and Mass Transfer, 2013, 63, 216-223.	4.8	33
54	Heat transfer and macrostructure formation of Nb containing TiAl alloy directionally solidified by square cold crucible. Intermetallics, 2013, 42, 184-191.	3.9	23

Jie-Ren Yang

#	Article	IF	CITATIONS
55	Thermal characteristics of induction heating in cold crucible used for directional solidification. Applied Thermal Engineering, 2013, 59, 69-76.	6.0	24
56	Uniformity analysis of magnetic field in an electromagnetic cold crucible used for directional solidification. COMPEL - the International Journal for Computation and Mathematics in Electrical and Electronic Engineering, 2013, 32, 997-1008.	0.9	4
57	Flow field and its effect on microstructure in cold crucible directional solidification of Nb containing TiAl alloy. Journal of Materials Processing Technology, 2013, 213, 1355-1363.	6.3	21
58	Effect of configuration on magnetic field in cold crucible using for continuous melting and directional solidification. Transactions of Nonferrous Metals Society of China, 2012, 22, 404-410.	4.2	11